CORUNDUM-BEARING VEINS IN CHLORITITE FROM THE ETIROL-LEVAZ AUSTROALPINE CONTINENTAL SLICE (VALTOURNENCHE, AOSTA, ITALY)

Roberto Compagnoni*,✉, Roberto Cossio* and **Daniele Regis****

  * *Dept. of Earth Sciences, University of Torino, Italy*.

** *Geological Survey of Canada, Ontario, Canada*.

✉ *Corresponding author, e-mail: roberto.compagnoni@unito.it*

ABSTRACT

The high-pressure (HP) continental Etirol-Levaz slice (ELS) is exposed on the right side of the Valtournenche (Aosta) at the contact between the overlying blueschist-facies Combin Zone and the underlying eclogite-facies Zermatt-Saas Zone. The ELS contains a layered metagabbro showing a complex evolution, which includes the pre-Alpine high-temperature (HT) recrystallization of the igneous mineralogies, and the polyphase Alpine metamorphism, initially at high-pressure (HP) quartz eclogite-facies, and later under greenschist-facies (GS) retrogression.

In this paper, unusual corundum-bearing ultramafic rocks associated with metagabbros are described. The studied sample is a Mg-chloritite with relict green spinel partly replaced by corundum, Mg-beltrandoite-2N3S (a new mineral of the högbomite supergroup), Mg-chlorite and dolomite. The rock is crossed by mm- to cm-thick veins composed of coarse-grained corundum + Mg-chlorite + dolomite. P-T phase-diagram projections indicate that the corundum-bearing assemblages formed in the presence of a water-rich fluid ($X(CO2) \leq 0.04$), during retrograde decompressional evolution. This stage follows the prograde HP-peak of the associated eclogites. The newly inferred prograde-to-retrograde P-T path suggests that the ELS and the underlying Zermatt-Saas Zone shared a common Alpine metamorphic evolution.

The detailed study of the relict minerals preserved in the chloritite indicates its pre-Alpine protolith, a green spinel websterite, and its evolution, characterized by a high-T recrystallization of the original igneous asemblages. During the Alpine orogeny, the spinel websterite experienced metasomatic hydration that converted the original igneous rock into a chloritite.

INTRODUCTION

Corundum (Crn) is a common mineral in a large variety of silica-undersaturated aluminium- and magnesium-rich metamorphic rocks such as metapelites and some impure marbles (e.g., Habler and Thöni, 2001; Riesco et al., 2005; Castelli et al., 2007; Gabudianu et al., 2009). Crn-bearing mafic and ultramafic rocks are rarer and most of them occur in peridotites as thin layers that mainly consist of garnet and clinopyroxene.

Crn has been reported from the ultramafic massifs of Beni Bousera, northern Morocco (Kornprobst et al., 1990), of Ronda (Morishita et al., 2001) and Cabo Ortegal, Spain (Girardeau and Gil Ibarguchi, 1991), and of the Sulu terrane, China (Zhang et al., 2004). Only few examples of Crn-bearing mafic/ultramafic rocks from the Alps have been described so far (e.g., Heinrich, 1982; Bucher-Nurminen et al., 1983; Müntener and Hermann, 1996; Braga et al., 2003) and none of them from the Western Alps.

Depending on the chemical composition of the rock, Crn is stable over a wide range of Temperature (*T*) and Pressure (*P*) conditions (e.g., Simonet et al., 2008). In the same range of *T* and *P*, Crn is often associated with minerals of the högbomite supergroup, a complex oxide family. Minerals of the högbomite supergroup have been reported as accessory phases from ca. 60 localities worldwide, mainly in metamorphosed Mg-Al-rich and metabasic rocks, from ~ 400ºC to > 700ºC (e.g., Grew et al., 1989; Petersen et al., 1989; Yalçin et al., 1993; Liati and Seidel, 1994; 1996; Razakamanana et al., 2000; Sengupta et al., 2004; 2009; Konzett et al., 2005).

In many localities minerals of the högbomite supergroup that mostly surround spinel suggest their formation from retrograde spinel-consuming reactions, such as: $Sp + Rt + H_2O \rightarrow Hög + Ilm$ (e.g., Friedman, 1952; Petersen et al., 1989; Tsunogae and Santosh, 2005). In the Western Alps corundum and högbomite have only been reported from a dolomite-rich impure marble of the Ultra-High-Pressure (*UHP*) Brossasco-Isasca unit (Castelli et al., 2007; Groppo et al., 2007).

Here we present the results of detailed petrochemical work undertaken on the first occurrence in the Western Alps of mafic/ultramafic rocks that contains Crn associated with a new mineral of the högbomite supergroup, named magnesiobeltrandoite-2N3S (Cámara et al., 2018). In the following, it is abbreviated as *Mg-Blt*, following the criteria suggested by Fettes and Desmons (2007). The investigated rocks are Crn-bearing chloritites from the layered metagabbro complex included in the Etirol-Levaz continental slice (Kienast, 1983).

Aluminium commonly behaves as a highly immobile element under sub-solidus conditions (e.g., Newton and Manning, 2008 and references therein), hence only small grains (< 1 mm) of corundum usually form during metamorphism. However, the formation of large crystals of Crn (> 1 mm) can be favoured by fluid-circulation in metasomatic processes especially in silica-undersaturated rocks (e.g., Yakymchuk and Szila, 2018). In the studied sample, Crn crystals are abundant and occur in both the chloritite matrix as fine-grained aggregates and in the veins as crystals from mm to cm in size (Fig. 2 and S2).
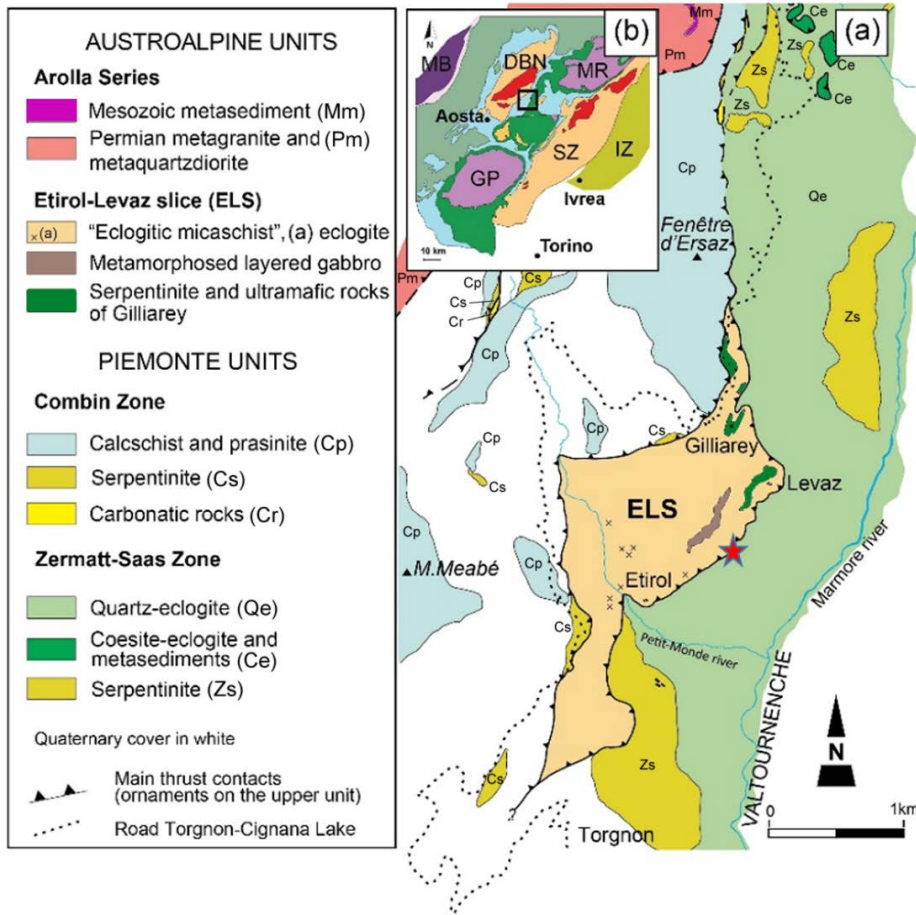
Fig. 1 - a) Geotectonic map of the continental Etirol-Levaz slice (ELS) and the adjoining units of the Piemonte Zone, modified after Kienast (1983) and Regis (2007). b) Simplified tectonic map of the northwestern Alps with location of the portion enlarged in Fig. 1a. <u>Southern Alps</u>: Ivrea zone (IZ, light green). <u>Austroalpine</u> of the Sesia Zone (SZ), the Dent Blanche Nappe (DBN) and other minor outliers in orange. In red the "second Diorito-Kinzigitic unit" of the Sesia Zone and the Valpelline Series of the DBN. <u>Piemonte Zone</u>: meta-ophiolites in green and metasediments ("calc-schists") in sky-blue. <u>Internal Crystalline Massifs</u> (purple) of Gran Paradiso (GP) and Monte Rosa (MR). <u>Grand Saint Bernard</u> basement and Briançonnais cover (grey). <u>Helvetic Domain</u>: Mont Blanc Massif (MB) in dark purple. The red star indicates where the studied samples were collected, i.e., in the debris just below the exposure in the ELS of the lens-like metamorphosed layered complex ("*Gabbros de Levaz*", in brown) mapped by Kienast (1983).
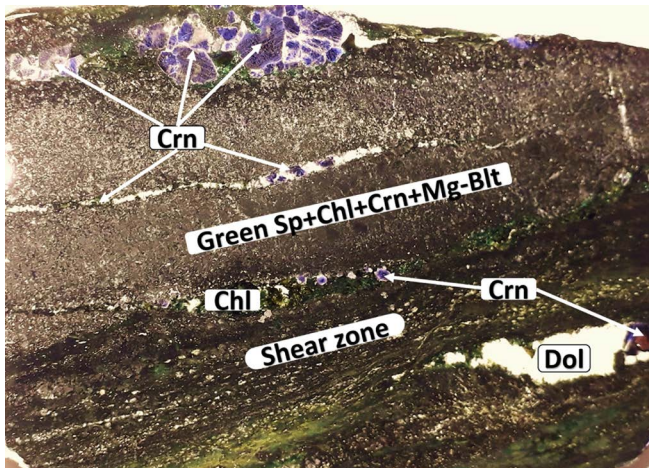
Fig. 2 - Polished slab of the studied chloritite sample cut perpendicular to foliation plane. The mineralogical banding and the grain-size variation are evident: The darker part in the middle preserves pre-Alpine relics of green spinel and Mg-Blt. Four veins parallel to foliation are evident for the presence of coarser grain-size corundum (Crn). The veins consist of different relative amounts of dolomite (white), Mg-chlorite (dark green) and corundum (Crn, blue). In the lower part, next to the dolomite-rich aggregate (Dol, white), a shear zone cuts the chloritite layer. Base of photo about 10 cm.

GEOLOGIC SETTING

The Etirol-Levaz continental slice (ELS), first reported by Hermann (1938), is exposed within the Piemonte zone on the right side of Valtournenche, Aosta Valley (Italy), less than 2 km to the south of the *UHP* Lago di Cignana Unit (e.g., Ballèvre et al., 1986; Regis, 2007; Beltrando et al., 2014). The ELS is exposed for ca. 4.5 km as a lens-like body, ~ 1 km thick in its central portion, sandwiched between the overlying blueschist-facies Combin zone and the underlying eclogite-facies Zermatt-Saas zone (e.g., Bearth, 1967; Dal Piaz and Ernst, 1978; Dal Piaz, 1999; Dal Piaz et al., 2001; Cartwright and Barnicoat, 2002); both of these meta-ophiolite units derived from the Mesozoic Piemonte-Liguria Ocean.

The ELS is mainly composed of garnet-phengite micaschists, also bearing omphacite (known as "eclogitic micaschists") and minor fine-grained phengite paragneisses, orthogneisses and small pods of eclogites locally retrogressed to prasinites (albite + chlorite + actinolite + epidote; Regis, 2007). Micaschists and gneisses derive from pre-Alpine, most likely Variscan, amphibolite- to granulite-facies paraschists and paragneisses, which are locally very well preserved (Kienast, 1983; Ballèvre et al., 1986). Within the micaschists, just below the Gilliarey Chapel close to the upper slice contact (Fig. 1), a small body of metaperidotites (olivine + Ti-clinohumite + relict Cr-spinel + magnetite + antigorite) is exposed (Regis, 2007). These metaperidotites have been interpreted either as part of the continental slice or as a fragment of a Zermatt-Saas ultramafic rocks, tectonically juxtaposed to the continental slice during the Alpine orogeny (Regis, 2007).

In the central portion of the ELS, a few hundred meters below the Gilliarey metaperidotites, a layered body of coronitic metagabbros with cumulus structures was reported by Kienast (1983), who studied in detail the reaction coronas developed around clinopyroxene, orthopyroxene, and spinel. Based on chemical compositions and microstructures of major phases, the author suggested that the layered metagabbros underwent an Alpine high-pressure metamorphic overprint at about 550ºC and 15-16 kbar.

A preliminary thermobarometric study on the high-pressure Alpine assemblages (garnet + omphacite + phengite + rutile) of two ELS eclogite samples (Regis, 2007) has shown a prograde *P-T* path characterized by two steps of garnet + omphacite growth. The metamorphic H*P* peak was constrained at ~ 560°C and ~ 24 kbar, at pressures significantly higher than the previous estimates (Kienast, 1983; Ballèvre et al., 1986), but very similar to the metamorphic peak of the adjacent Zermatt-Saas Zone at Lago di Cignana, i.e., ~ 600°C and ~ 24 kbar (Bucher et al., 2005; Groppo et al., 2009).

Only few geochronological studies have been undertaken on the ELS. Dal Piaz et al. (2001) obtained a phengite Rb-Sr age of 45-47 Ma for the H*P* metamorphic stage. More recently, zircons from an orthogneiss sample, collected at the bottom of the ELS close to the contact with the underlying Zermatt-Saas zone, dated by ion-probe (Beltrando et al., 2010 a and b) gave a Permian age for the magmatic cores and a Jurassic age (166-150 Ma) for the overgrown rim. This Jurassic age has been interpreted as related to the infiltration of melts associated to the intrusion of oceanic mafic magmas, suggesting that the continental rocks of the ELS were already juxtaposed to the oceanic basement (Beltrando et al., 2010b). Therefore, the slice has been considered as an extensional allochthon, derived from the Adriatic continental margin and stranded inside the Piemonte-Liguria oceanic domain during the Jurassic rifting (Dal Piaz et al., 2001; Beltrando et al., 2010b). The Alpine peak-to-retrograde eclogite-facies overprint, dated on the same zircon crystals (47.5 ± 1.0 Ma SHRIMP U/Pb zircon: Beltrando et al., 2010b), confirms the Rb-Sr data of Dal Piaz et al. (2001).

METHODS

Sampling

As the layered complex is exposed on an almost inaccessible wall, two samples were collected at the base of the cliff, a *chloritite* for its unusual composition and mineralogy, and a *metagabbronorite* of the layered complex described by Kienast (1983) for comparing the metamorphic evolution.

Analytical methods

For major elements analyses a Cambridge S-360 SEM, equipped with Oxford Instruments Inca Energy 200 EDS spectrometer and X-Act3 SDD detector, was used at the Department of Earth Sciences, University of Turin. All measurements were performed on carbon coated thin sections, using oxides and minerals as standards (SPI) and Oxford Instruments quantitative XPP correction. The analytical conditions were: beam energy of 15 keV, current probe of 1nA, take-off angle of 35 deg, each EDS spectrum (1024 channels, 10 eV/ch) with about $4 * 10^5$ counts.

For minor elements analyses, we used an Eagle III XPL Micro-X-ray Fluorescence (μ-XRF) Spectrometer at Dept. of Earth Sciences, the University of Torino, equipped with Rh X-ray tube, poly-capillary (spot size = 30 μm), six primary filters and Si ultrapure EDS thick Be window detector. All measurements were performed in vacuum, using Fundamental Parameters correction. The analytical conditions include: Rh X-ray tube (excitation at 40 kV, 1 mA) with Ni 25 μm thick primary filter. This configuration in general attenuates the light elements, but at the same time it allows to use the full power of the X-ray tube and increases sensitivity in certain regions of the spectrum (depending on the primary filter used) corresponding to the analytical line of elements of interest.

For the Crn trace-element composition profile, a 2.1 mm long line with 64 points (step = 33 μm) and 15 *s* live time for each spectrum was selected. At these conditions, for ~ 1000 ppm concentration of Ti and Cr, the relative statistical error is about 5%.

All mineral phases from both matrix and veins contain chromium as confirmed by the presence of a doublet in the luminescence spectra, well known in the ruby (lines R1 = 694.5 nm and R2 = 693.0 nm), where Cr^{3+} substitutes for Al (see e.g., Gaft et al., 2005). This doublet is evident not only in the luminescence spectra of minerals with chromium detectable at SEM-EDS or at X-ray micro-fluorescence (i.e., in the range 0.5 - 1.5 wt%, such as corundum, green spinel and Mg-beltrandoite) but also in phases with Cr-content lower than the detection limit (i.e., lower than 0.1 wt%), such as chlorite, magnesite, dolomite and calcite: Fig. S1).

Structural formulae of analyzed minerals were calculated on the basis of 3 cations and 4 oxygens for spinel, 28 cations and 40 oxygens for Mg-beltrandoite-2*N3S* (see Cámara et al., 2018), 2 cations and 3 oxygens for corundum, 20 cations and 28 oxygens for chlorite and 6 oxygens for carbonates (dolomite, magnesite and calcite).

PETROGRAPHY AND MINERAL CHEMISTRY

Chloritite

The chloritite sample is a banded and foliated rock that consists of alternating layers of variable thickness, grain size and mineralogy (Fig. 2). Four layers, characterized by coarser grain-size bluish corundum (Crn in Fig. 2), are veins that consist of varying relative amounts of dolomite (white), Mg-Chl (dark green) and Crn (blue) (Fig. 3b-d). The darker layer in the middle of the sample (marked in Fig. 2 by a string of mineral abbreviations) consists of fragmented porphyroclasts of green spinel surrounded by a finer-grained matrix (Fig. 3a) that includes colourless Dol (white), red-brown Mg-Blt, Mg-Chl and sparse Crn. The other layers mainly consist of chlorite that defines the rock foliation. In the lower part of the sample (Fig. 2) a shear zone is evident, which is characterized by the development of a mylonitic foliation with grain size reduction. On the upper surface of the hand specimen roughly parallel to foliation, the hard Crn porphyroblasts stand out on the much softer chlorite matrix (Fig. S2), and appear as knots of deep blue colour with light pink portions.

Corundum

In thin section, the vein Crn shows a patchy zoning with either deep blue (ε = pale greenish blue, ω = deep blue, absorption: ε < ω) or colourless portions, corresponding to the pink coloured portions observed in hand specimen (Fig. S2). In addition to growth zoning, the blue Crn becomes colour-

less also along cracks, now marked by strings of former fluid inclusions (Fig. 3d). It is evident that this discoloration process, which has an average penetration of ca. 50 μm on both sides of the fracture, was produced by leaching of the chromophore elements by circulating fluids (see below). Some Crn crystals show lamellar twinning on $\{10\bar{1}1\}$.

Crn shows a variety of habits against the associated minerals. It is anhedral with respect to chlorite (Fig. 3b), which suggests a partial replacement, as evident also at small scale (Fig. S3a), but euhedral against dolomite (Fig. 3c). Along fractures and cleavage planes, Crn is partially converted to diaspore (Figs. S3b).

To identify the nature of the chromophore elements (see e.g., Giuliani et al. 2007, with references therein), a chemical profile across a representative zoned Crn crystal was analyzed by micro-XRF (Fig. 4). The element profile shows that the central colourless (pink in hand specimen, Fig. S1) portion corresponds to a drastic drop in TiO_2 from 0.15-0.2 wt% in the blue portions to values below the detection limit. This decrease in TiO_2 is coupled with an increase in Fe_{tot} from ca. 0.9 to 1.3 wt%, whereas the value of Cr_2O_3 is almost constant (~ 0.1 - 0.2wt%) from core to rim. In accordance with litera-

ture data (see e.g., Emmett et al., 2003, with refs. therein), it may be suggested that the blue colour is due to the well-known substitution of Al^{3+} by iron (Fe^{2+} or Fe^{3+}) and titanium (Ti^{4+}) by a mechanism of intervalence change transfer between metal ions (Fe^{2+} - O - Ti^{4+}) in the crystal lattice. The pale pink colour of the portions colourless in thin section may be ascribed to the higher Cr^{3+} content, coupled with the drop of titanium, responsible with iron for the deep blue colour.

Magnesiobeltrandoite

In a previous short paper, this mineral was identified as högbomite, based on the optical properties (Regis et al., 2015). However, a deeper and more accurate re-examination based on EMPA analyses combined with a single-crystal X-ray study allowed identifying this mineral as a new member of the högbomite supergroup. This oxide family is related to the spinel group but differs from it by having variable contents of TiO_2 and structural hydroxyl (e.g., Grew et al., 1989; Petersen et al., 1989; Armbruster, 2002; Hejny and Armbruster, 2002; Tsunogae and Santosh, 2005). The complex modular structure of this family, composed of nolanite (N = $TM_4O_7(OH)$) and spinel (S = $T_2M_4O_8$) modules, where T and
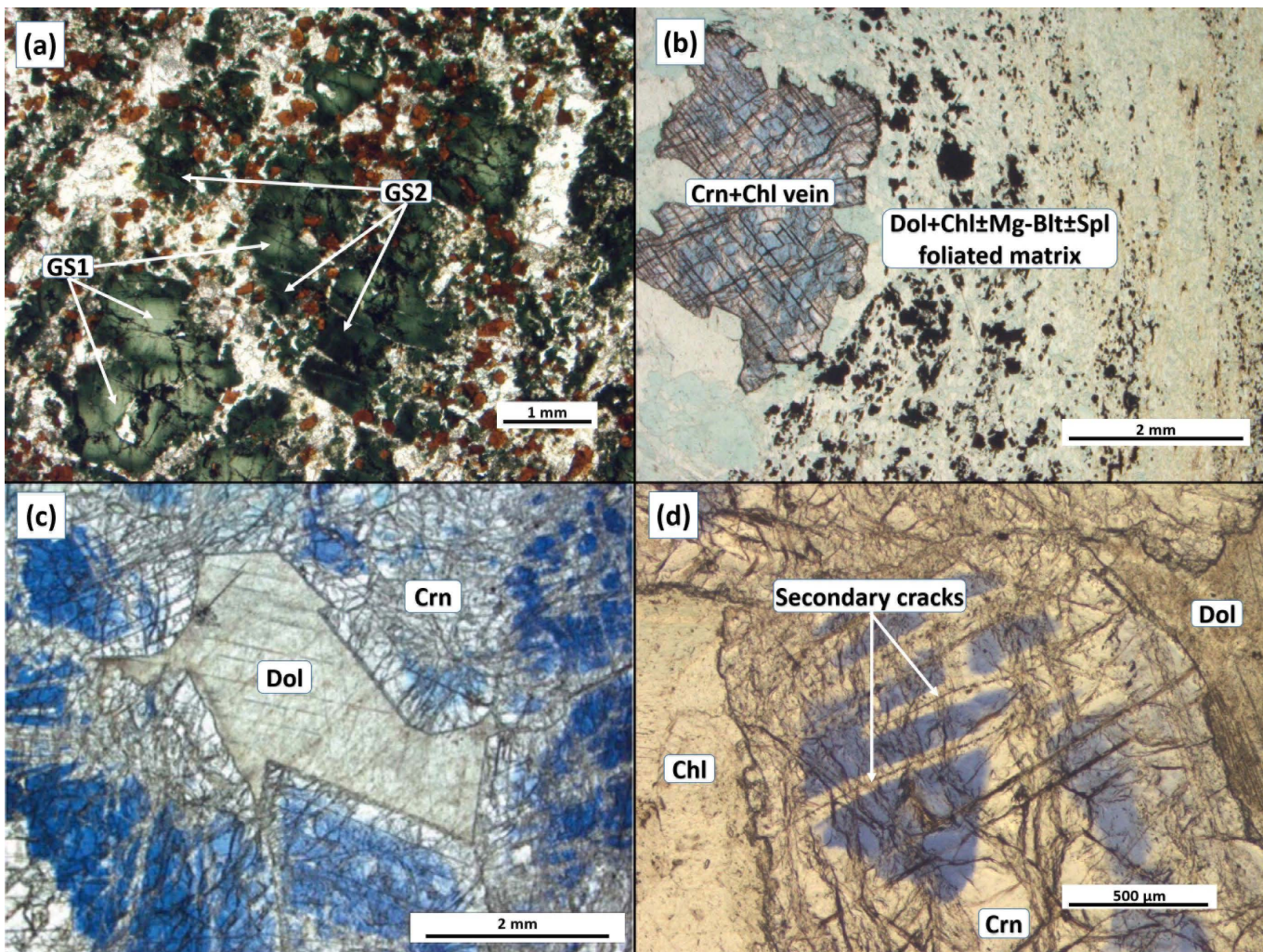
Fig. 3 - a) Photomicrograph of the relict portion of the chloritite with corroded fragments of zoned green spinels (pale green igneous GS1, and dark green metamorphic GS2) and red-brown Mg-Blt are embedded in a finer-grained matrix of prevailing dolomite. b) Photomicrograph of a coarse-grained Crn + Chl (± Dol) vein, surrounded by a foliation defined by chlorite with black crystals of Mg-Blt ± relict green spinel (Spl). Note the large Crn porphyroblast corroded by chlorite. PPL; c) Photomicrograph of a vein Crn with patchy colour zoning. Note the euhedral habit of Crn against Dol. PPL; d) Photomicrograph shows the original blue colour bleached by late fluids leaching chromophore elements along cracks. PPL.

M represent tetrahedrally and octahedrally coordinated cations, respectively, may form different polysomes depending on the succession of the layers. The new mineral was named *magnesiobeltrandoite-2N3S*, where the suffix indicates the polysomatic sequence, consisting of two nolanite (*N*) modules alternating with three spinel (*S*) modules (Cámara et al., 2018); its ideal formula $Mg_6Al_2(Al_{18}Fe^{3+}_2)O_{38}(OH)_2$. Mg-Blt is isostructural with magnesiohögbomite-2*N3S*.

In thin section, the Mg-Blt crystals cannot be distinguished from magnesiohögbomite, having the same optical properties (high relief, uniaxial negative sign, pleochroism with ε = deep-orange and ω = brownish red) and trigonal prismatic crystal habit. The average size of Mg-Blt is in the range 0.2-1.0 mm, but smaller crystals may also be found. Euhedral prismatic crystals occur both as inclusions in relict green spinel GS2, whereas smaller corroded crystals are found in the matrix surrounding the green spinel porphyroclasts (Fig. 3a). Much like green spinel, Mg-Blt often exhibits fractures sealed with dolomite + chlorite ± corundum, i.e. the vein minerals (Fig. 5). Because of such microstructural observations, Mg-Blt is considered a H*T* mineral coeval with green spinel GS2. Mg-Blt is slightly zoned with X_{Mg} (Mg/(Mg+Fe$_{tot}$)) ranging from 0.5 in the core to 0.3 in the rim (Fig. 5, Table S1), and titanium enriched in the core (TiO$_2$ ~ 1.5 wt%), while in the rim TiO$_2$ is often below detection limit (bdl). Some smaller (< 50 μm) xenoblastic Mg-Blt crystals have higher titanium (TiO$_2$ = 2-4 wt%) and iron (FeO = and 25-26 wt%) concentrations (Fig. 5, Table 1).

Spinels

Green spinel occurs as coarse-grained porphyroclasts up to several mm across (Fig. 3a), usually fragmented with fractures filled by a fine-grained assemblage of Mg-Blt, dolomite, chlorite and rare Crn (Fig. 3a). As evident from the photomicrograph (Fig. 3a), spinel is clearly zoned with a pale green core (GS1) extensively re-equilibrated to a dark green one (GS2).

From SEM-EDS data, green spinels are mainly solid solutions of Hercynite (FeAl$_2$O$_4$) and Spinel (MgAl$_2$O$_4$) (Bosi et al., 2019). GS1 has a composition close to Sp$_{58}$Hc$_{42}$, whereas GS2 close to Sp$_{35}$Hc$_{65}$ (Fig. 6 and Table S1). Minor zoning in Cr is observed with values ranging between 0.002 apfu in the core of GS1 up to 0.200 apfu in the rim of GS2. Local inclusions of euhedral Mg-Blt were observed in spinel, but only in GS2 (Fig. 3a).

Chlorite

Chlorite occurs as both mm-sized flakes in the rock matrix and larger crystals in the metamorphic veins, where it is in equilibrium with dolomite and corundum (Fig. 8c, Table 1). In the rock matrix the chlorite cores are enriched in Mg (X_{Fe} = 0.10-0.15, *sheridanite* according to Hey 1954, Fig. 7c), compared to the silica-depleted rims (X_{Fe} = 0.25-0.30, *corundophilite* according to Hey 1954, Fig. 7c). The chlorite crystals of the veins show the same compositional variation and trend.

Carbonates

Carbonates are abundant (> 20 vol%) in the analyzed thin sections (Table 1). The most common carbonate is *dolomite*, which occurs both in the rock matrix, associated with chlorite and corundum, and in the veins as coarser crystals together with corundum and Mg-chlorite (Fig. 3 b and c). Dolomite is locally replaced by *calcite* along cleavages and fractures. Rare relics of *magnesite* were observed within the dolomite crystals of the matrix.
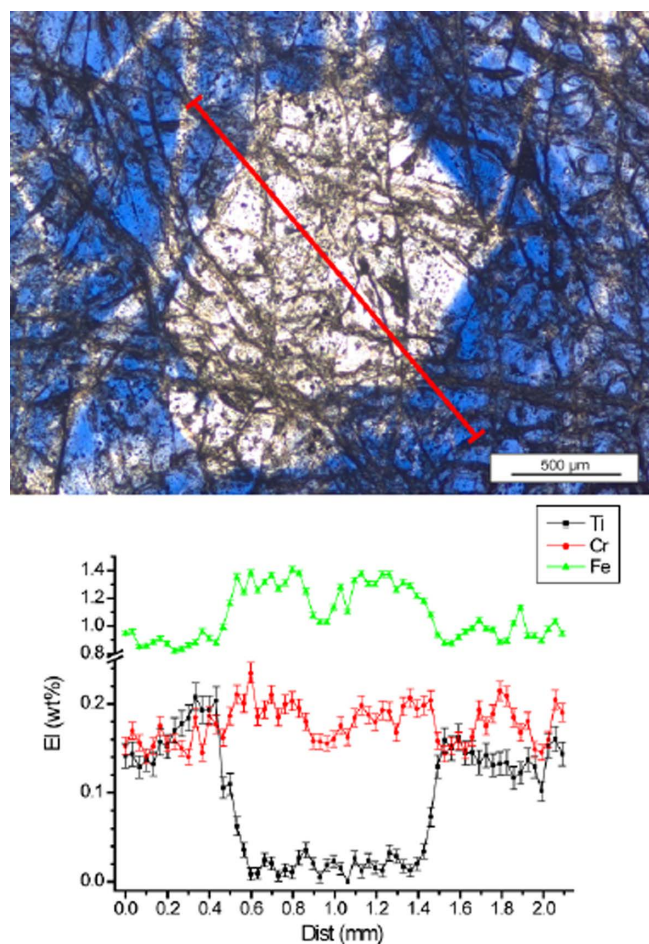
Fig. 4 - X-ray microfluorescence elements profile across the growth zones of a typical vein corundum (see Fig. 3c). See text for explanation.
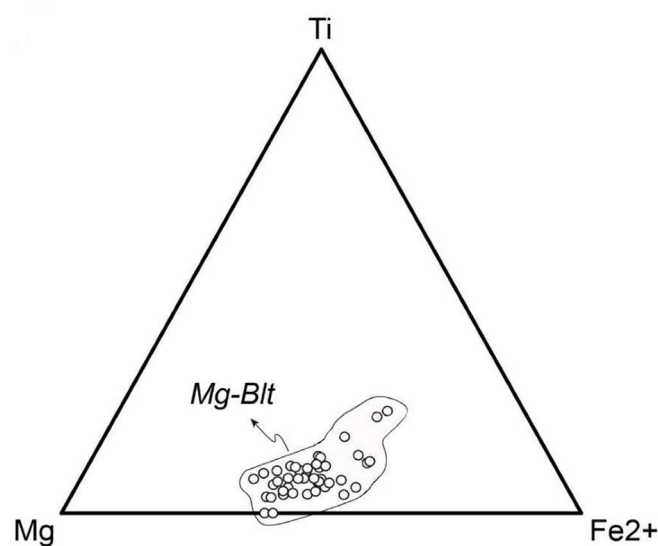
Fig. 5 - Compositional variation of magnesiobeltrandoite (Mg-Blt) plotted in the Mg-Fe^{2+}-Ti ternary endmember diagram.

(a)

(b)
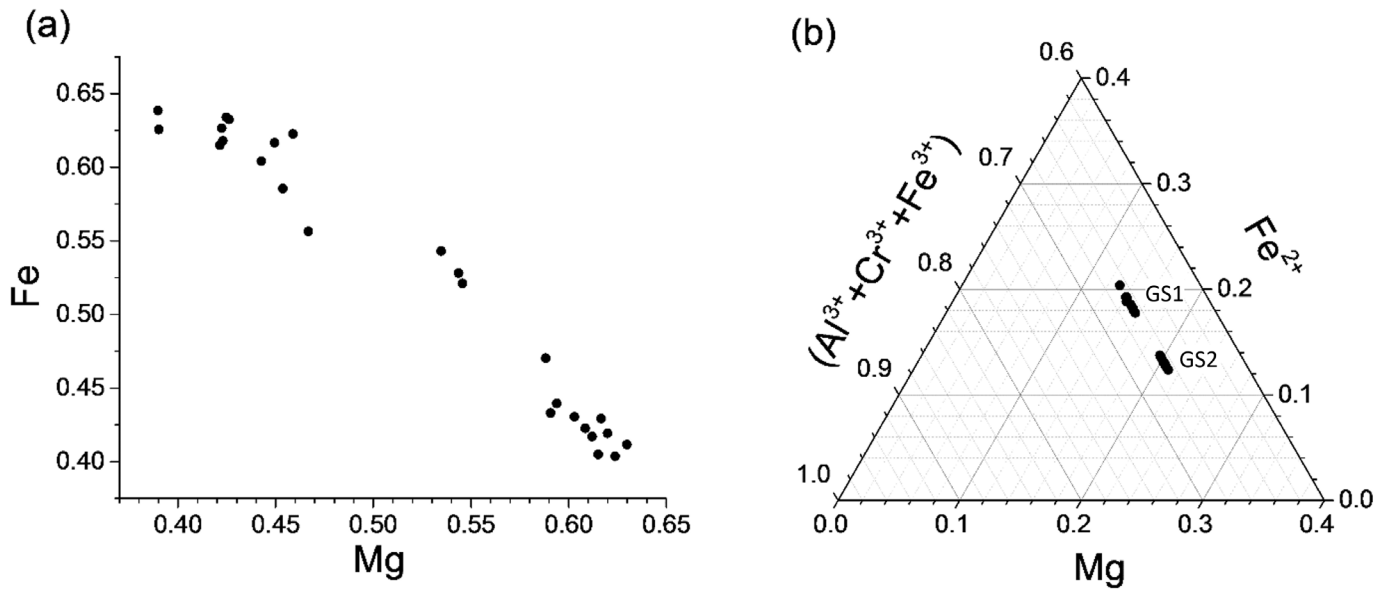
Fig. 6 - a) Fe vs Mg diagram of the spot analyses of green spinel illustrates the wide zoning range. b) Selected analyses show an enrichment in iron and decrease in Mg from GS1 to GS2, respectively, at a constant content of trivalent ions. Molar units used in both plots.

Opaque minerals

Hematite with skeletal habit locally occurs, filling a network of late fractures. Iron sulphides with S/Fe ratio around 1:1 - most likely *pyrrhotite* - are also present, but their geometric relationships with the other minerals are difficult to infer.
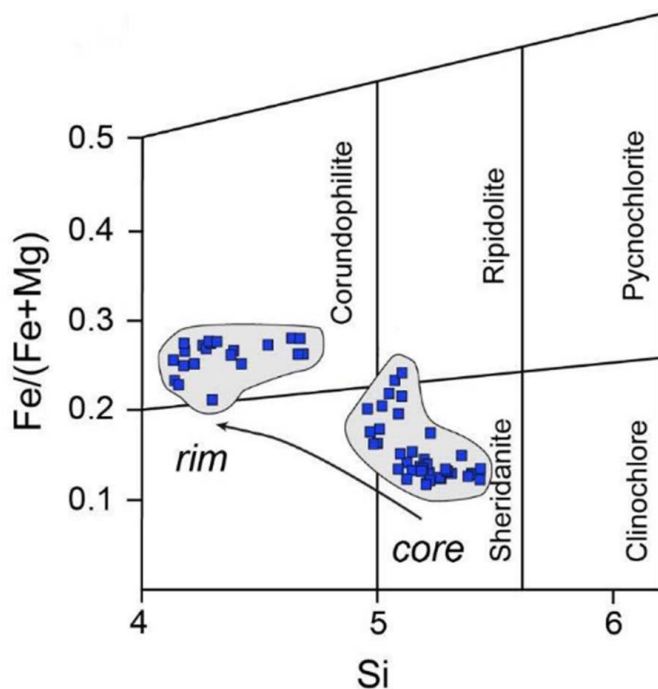
Fig. 7 - Classification diagram of chlorites (Hey 1954) shows a compositional gap, characterized by Fe^{2+} increasing and a Mg decreasing from core to rim in both matrix and vein chlorites.

Metagabbronorites

As described by Kienast (1983), to whom we refer for a more exhaustive description, the metagabbros of the layered complex are characterized by portions with coarser grain-size and higher modal amounts of plagioclase (up to 50 vol%). The studied sample is a *metagabbronorite* (Figs. 8 a-d) mainly consisting of clinopyroxene (Cpx), orthopyroxene (Opx), former plagioclase (ex-Pl) and black spinel (Sp). Opx forms larger crystals with fine exsolution lamellae of Cpx (Figs. 8 a and b), whereas the Cpx occurs as finer-grained granoblastic polygonal aggregates. Since the metagabbros preserve the original igneous fabric, it may be concluded that unlike Opx, which is still the igneous phase, the neoblastic Cpx aggregate has recrystallized at the expense of the original igneous pyroxene, as already suggested by Kienast (1983). This partial H*T* recrystallization of the igneous minerals is followed by the polyphase Alpine evolution. During the early H*P* metamorphism the H*T* phases were partially to completely replaced by the following pseudomorphous to coronitic reactions (Kienast, 1983): Pl → Na-Cpx + Zo ± Ky; Opx → Tlc + Grt ± Ky ± Mg-Chl; Cpx → Omp + Grt + Tlc ± Amp ± Prg ± Phe; Sp → Chl (Mg-Chl) + Crn + Dol ± Grt. In our sample, the Alpine H*P* re-equilibration leads to the igneous plagioclase pseudomorphically replaced by jadeitic pyroxene + zoisite ± quartz (Figs. 8 a and b) and to the partial alteration of black spinel to Mg-Blt, Crn, Chl and Dol (Fig. 8 c and d).

The layered complex experienced a polycyclic evolution, unevenly distributed among lithologies (Table 1). In the studied metagabbronorite the post-magmatic H*T* event is mainly evident by the recrystallization of igneous Cpx into a granoblastic aggregate, and by the occasional occurrence of Mg-Blt (Figs. 8c and d). The early Alpine event is evident in the widespread H*P* pseudomorphous and coronitic reactions after igneous minerals, as carefully documented by Kienast (1983). The chloritite, having experienced an important metasomatic process, preserves only few relics of its long history: GS1 as a remnant of the original igneous protolith, GS2 and Mg-Blt as remnants of the H*T* metamorphic event, and the assemblage Crn + Chl + Dol as evidence of the Alpine H*P* event (Table 1).
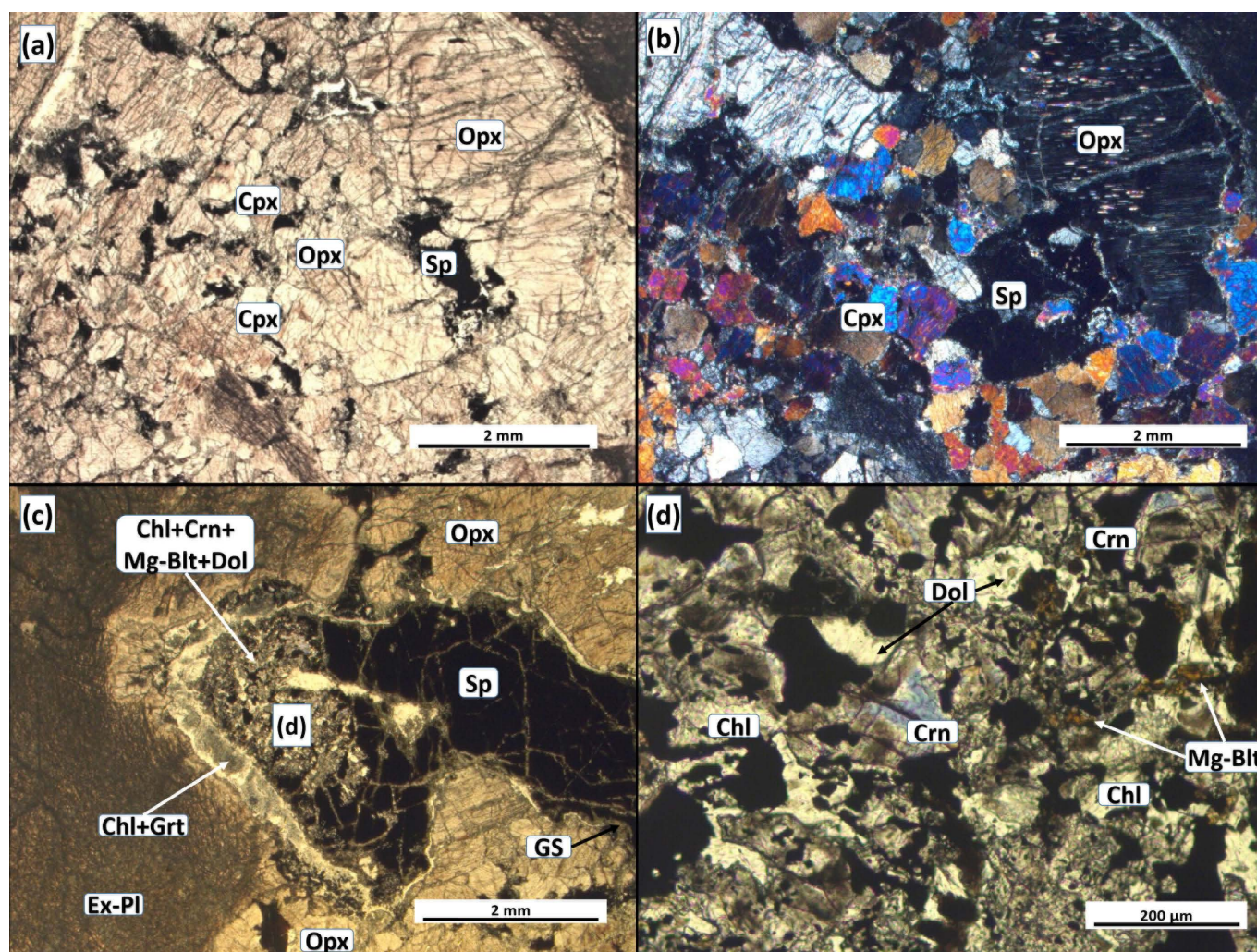
Fig. 8 - a) Photomicrograph of an undeformed metagabbronorite from the layered complex with igneous orthopyroxene (Opx), clinopyroxene (Cpx) and black spinel (Sp). The dark aggregate in the upper right corner is a Na-Cpx + Zo pseudomorph after igneous plagioclase. PPL; b) The same photomicrograph taken at crossed polarizers shows the original igneous Opx with Cpx exsolutions, and the polygonal granoblastic aggregate of Cpx recrystallized over igneous Cpx. XP; c) Photomicrograph of a metagabbronorite that shows the original igneous spinel (Sp) partly replaced by a fine-grained mineral aggregate enlarged in Fig. 8d (white box labelled d). Note the Grt + Chl reaction corona of partly chloritized (Chl) garnet (Grt) developed at the contact between the igneous plagioclase (now Na-clinopyroxene + Zoisite) and the black spinel. Cf.: Kienast (1983). PPL; d) Photomicrograph of the enlarged portion white and labelled (d) in Fig. 8c, that shows the alteration products of black spinel, including Mg-Blt, Crn, Chl, and Dol. PPL

Table 1 - Petrographic evolution of the metagabbronorite and the Crn-bearing chloritite from the Etirol-Levaz continental slice.

| Lithology | Magmatic | Metamorphic | | |
	Igneous assemblage	Pre-Alpine HT-LP assemblage	Alpine HP assemblage	Alpine LP assemblage
Gabbronorite	Cpx I	Cpx II	Omp + Grt + Tlc ± Amp ± Prg ± Phe	Fe-richer-Chl + Cal
	Opx I	Opx II	Tlc + Grt ± Ky ± Mg-Chl	
	Pl I	Pl II	Na-Cpx + Zo ± Ky	
	Spl (black)	Spl (green) + Mg-Blt	Mg-Chl + Crn + Dol ± Grt	
Chloritite (from former Spinel websterite)	Green spinel (GS1)	Green spinel (GS2) Mg-Blt Mgs (?)	Crn + Dol + Mg-Chl	Fe-richer-Chl + Dsp + Cal

Metagabbronorite data mainly from Kienast (1983). Mineral abbreviations- Amp: amphibole, Cal: calcite, Chl: chlorite, Cpx: clinopyroxene, Crn: corundum, Dol: dolomite, Dsp: diaspore, Grt: garnet, GS: green spinel, Mg-Blt: magnesiobeltrandoite, Ky: kyanite, Na-Cpx: jadeite-rich pyroxene, Omp: omphacite, Opx: orthopyroxene, Phe: phengite, Pl: plagioclase, Prg: paragonite, Spl: spinel, Tlc: talc, Zo: zoisite.

Petrogenetic grid in the CMAS-H$_2$O-CO$_2$ system

In order to estimate the *P-T-X$_{(CO2)}$* conditions during the Alpine evolution, characterized by the vein assemblage chlorite + corundum + dolomite, the chloritite was investigated by projecting variable volatile compositions along univariant equilibria of a *P-T* phase diagram whose variations of fluid composition and mineral assemblage can be predicted (e.g., Baker et al., 1991; Carmichael 1991; Connolly and Trommsdorff, 1991; Omori et al., 1998; Castelli et al., 2007). Because the Crn-bearing chloritite is largely dominated by CaO-MgO-Al$_2$O$_3$-SiO$_2$-H$_2$O-CO$_2$, the system CMASHC was selected for simplicity using the computational approach of Connolly (1990) and Connolly and Trommsdorff (1991) (Perple_X version 6_6_8) with the thermodynamic data and the equation of state for H$_2$O-CO$_2$ fluids of Holland and Powell (1998, revised 2004). The solid endmembers used for the calculation were: anorthite, aragonite, calcite, chlorite, corundum, dolomite, diaspore, magnesite, spinel and zoisite. Anorthite and zoisite were included in the calculations to account for the presence of Al-rich phases at different stages of the retrograde evolution (see e.g., Castelli et al., 2007). The thermodynamic properties of spinel (Spl* = Sp$_{50}$, Figs. 6 and 9) and chlorite (Chl* = Clin$_{80}$, Figs. 7 and 9) were modified to match the actually analyzed compositions (Fig. 9); this allows changes in their *P-T-X$_{(CO2)}$* stability fields to be modeled. Quartz and coesite were excluded because of the presence of spinel that indicates a Si-undersaturated rock chemistry. The presence in the *P-T* projection of univariant curves with abrupt terminations is due to the exclusion of reactions involving quartz and coesite.

The grid was calculated from 1.0 to 40.0 kbar and from 400 to 900ºC (Fig. 9). In the calculated petrogenetic grid, 35 fluid-present and 7 fluid-absent univariant reactions generate 14 fluid-present invariant points (Fig. 9). Three of the 35 fluid-present univariant curves are characterized by the presence of singular points where the amount of one of the reactants is reduced to zero and on both sides of the point mineral changes side in the reaction (see e.g., Abart et al., 1992). The
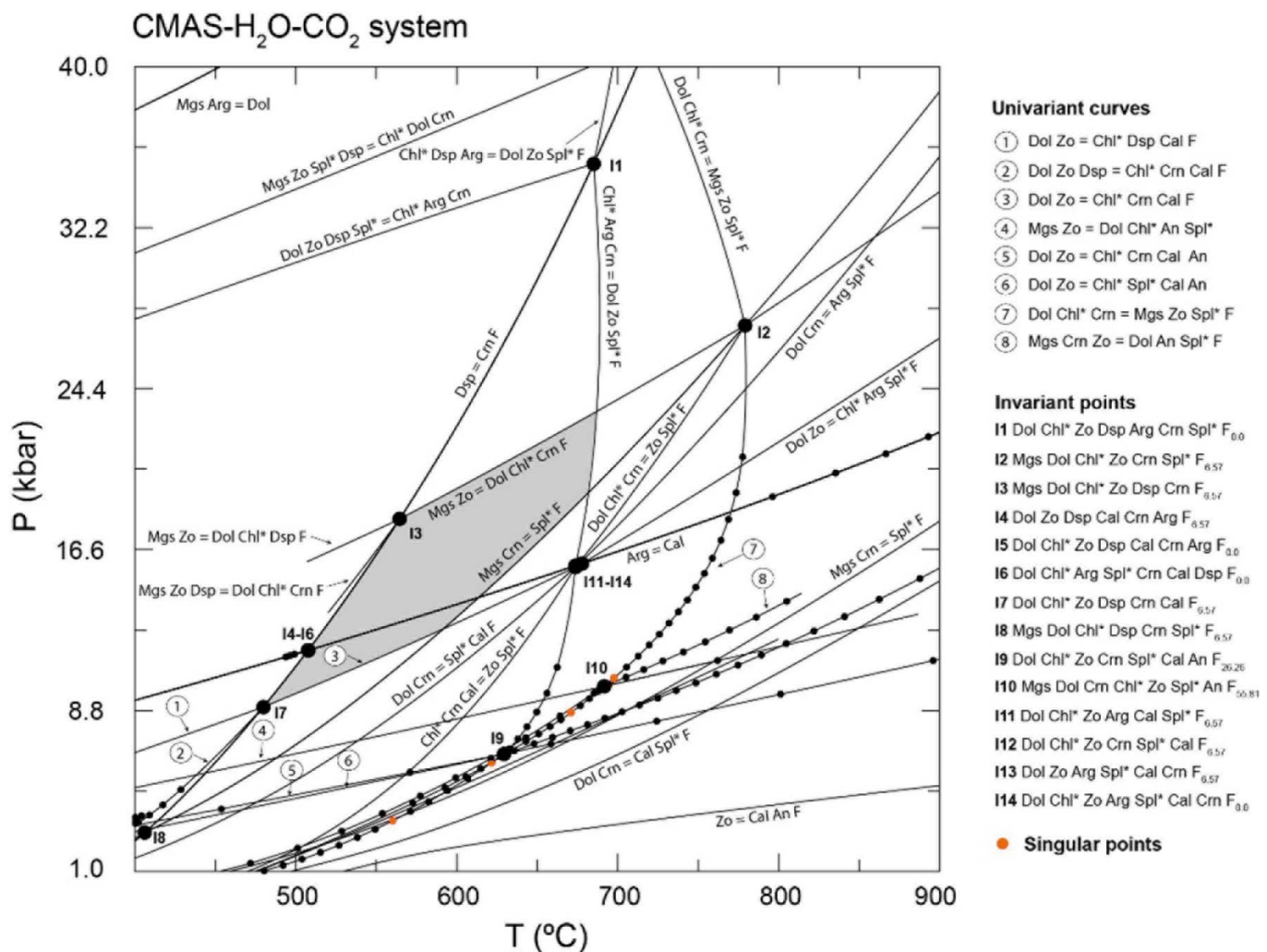
Fig. 9 - Petrologic modeling of Alpine mineral reactions in the CMAS-H$_2$O-CO$_2$ system. Grey field: stable assemblage in the matrix and veins (Dol + Chl* + Crn + Fluid). Mg-Blt not included in the modelling for lack of thermodynamic data. * refers to the phases for which thermodynamic properties were changed to match the real analyzed composition: Spl* (*sp50*) = MGO(1)AL2O3(1), G0 = -2177728. S0 = 87.26311 V0 = 3.978 c1 = 242.7 c2 = -.6037E-2 c3 = -2315100 c5 = -1678.1 b1 = .431E-4 b5 = -.431E-3 b6 = 2118971. b7 = -291.75 b8 = 4; Chl* (*clin80)* = MGO(5)AL2O3(1)SIO2(3)H2O(4), G0 = -8252373. S0 = 432.3553 V0 = 21.09 c1 = 1161.8 c2 = .10133E-1 c3 = -7657300 c5 = -9690.899 b1 = .398E-4 b5 = -.398E-3 b6 = 947817.1 b7 = -130.5 b8 = 4. Abbreviations: An- anorthite, Arg- aragonite, Cal- calcite, Chl- chlorite, Crn- corundum, Dol - dolomite, Dsp- diaspore, F- fluid, Mgs- magnesite, Spl- spinel, Zo- zoisite.

singular points were found along the Dol-Chl*-Cor-Mag-Zo-Sp*-F, Dol-Crn-Chl*-Zo-Sp*-An-F and Dol-Crn-Chl*-Sp*-An-Cc-F univariant curves. The fluid-present univariant curves intersect in several points and dissect the *P-T* space into narrow regions, some of them relevant for deciphering the peak-to-retrograde evolution of the samples.

The observed Alpine assemblage Crn-Chl*-Dol-F is constrained to the range 8.5-21.5 kbar and 480-670°C (Fig. 9). For the same system, a T-$X_{(CO2)}$ section was calculated at 17 kbar in order to better constrain the fluid composition in equilibrium with the assemblage Crn-Chl*-Dol-F (Fig. 10). For $T < 600°C$ (compatible with the evolution of the ELS) the fluid composition in equilibrium with the assemblage Crn-Chl*-Dol is approximated by a composition with $X_{(CO2)} \leq 0.04$ (Fig. 10).

DISCUSSION

P-T-$X_{(CO2)}$-t evolution

Phase-equilibria, derived from the petrogenetic grid calculated in the CMAS-H_2O-CO_2 system, can be used to infer the retrograde evolution of the corundum-bearing chloritite. The metamorphic *P-T* path of the studied samples, constrained by linking the observed microstructural relationships among major- and minor-phases, mineral chemistry and phase-equilibria modeling, is shown in Fig. 11.

The Etirol-Levaz continental slice is mainly composed of garnet-phengite micaschists and fine-grained phengite gneisses with layers and/or boudins of eclogites. These have locally been retrogressed to prasinites, but a mafic layered complex was reported and mapped by Kienast (1983) in the core of this slice. An orthogneiss sample, collected at the bottom of the Etirol-Levaz slice just at the contact with the underlying Zermatt-Saas antigorite serpentinites, has been the subject of high-precision *in-situ* geochronology by Beltrando et al. (2010a). The dated zircons show Permian magmatic cores overgrown by Jurassic (166-150 Ma) rims. This age, interpreted as the result of melt infiltration associated with the intrusion of rift-related gabbroic magmas, indicates that the continental slice was already juxtaposed to the oceanic basement prior to the Alpine orogeny. The Alpine eclogite-facies overprint of the Etirol-Levaz continental slice, dated at 47.5±1.0 Ma (SHRIMP U/Pb zircon: Beltrando et al., 2010b), shows a prograde path peaking at 2.4 GPa and 550°C (Regis, 2007; Fig. 11), which overlaps the Alpine high-pressure metamorphic peak and evolution estimated for the Zermatt-Saas tectonic unit overlying the UHP Lago di Cignana unit (Groppo et al., 2009).

During the later metamorphic evolution, the most typical Alpine assemblage in the chloritite investigated is represented by Dol + Chl + Crn. In the CMAS-H_2O-CO_2 system, these phases are stable in the grey area of Fig. 11, which is delimited by five fluid-present reactions. At higher pressure ($P \leq 20$ kbar) the mineral assemblage is formed by the uni-
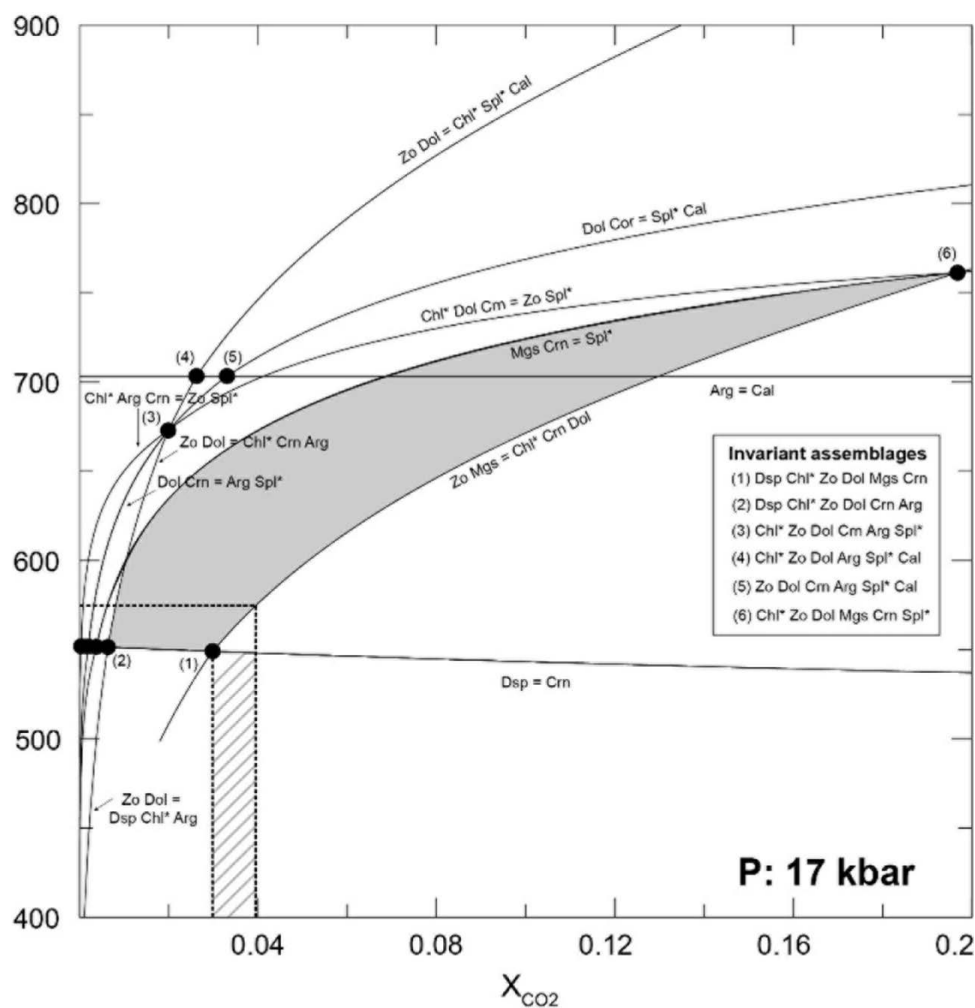
Fig. 10- Isobaric (at 17 kbar) T-$X_{(CO2)}$ diagram of the assemblage Dol + Chl* + Crn (cf. Fig. 9). The inferred metamorphic T (in the range 550-600°C) are consistent with the published estimates for the eclogite-facies Zermatt-Saas Zone of the Piemonte unit. For these temperatures the composition of the fluid phase in equilibrium with the observed assemblages is constrained to be dominantly hydrous ($X_{(CO2)} \leq 0.04$). Three invariant assemblages not listed.

variant reaction (i) Mag Zo = Dol Chl* Crn F (Fig. 11). The high temperature curves ($T \leq 680°C$), delimiting the field of interest, involve the crystallization of spinel and consumption of corundum according to reaction (ii) Chl* Arag Crn = Dol Zo Sp* F and (iii) Mag Crn = Sp* F. At lower pressure ($P \leq$ 11 kbar), the calcite stability is limited by reaction (iv) Dol Zo = Chl* Crn Cc F; at lower temperatures ($T \leq 550°C$), a limiting reaction involves diaspore according to reaction (v) Dsp = Crn F.

The retrograde phases calcite and diaspore, derived from reactions (iv) and (v), have been observed in all samples, while the reactants are not always preserved. According to the modeled grid, zoisite is involved in two reactions forming dolomite (i) and calcite (iv), respectively. The absence of zoisite in thin section probably indicates complete consumption during the two decompression reactions. Magnesite, involved in reaction (i), is locally preserved as small inclusions in large dolomite crystals.

In summary, microstructures and modeling of phase equilibria indicate that formation of the Alpine assemblage (Dol + Chl + Crn) in both the matrix and the Crn-bearing veins occurred at ~ 17-15 kbar and ~ 580°C (Fig. 11) in the presence of a fluid characterized by low $X_{(CO2)}$ (≤ 0.04: Fig. 10). This HP stage was followed by decompression and cooling involving the replacement of dolomite by calcite (Cc-in: reaction (iv), Fig. 11) and of corundum by diaspore (Dsp-in: reaction (v), Fig. 11).

The reconstructed P-T path fits well with the ELS prograde to peak Alpine metamorphic conditions estimated from the eclogite layers preserved within micaschists (Regis, 2007). These eclogites are characterized by a two-stage prograde evolution from ~ 520°C and 20 kbar (step A, Fig. 11) to peak conditions of ~ 560°C and 24 kbar (step B, Fig. 11). These data suggest that the Crn-bearing assemblage should have formed during post-peak decompression at lower temperatures and pressures (Fig. 11) but in continuity with the HP peak trajectory. Moreover, the reconstructed path overlaps the P-T evolution estimated for the adjacent "upper eclogite-facies unit" of the Zermatt-Saas zone (e.g., Bucher et al., 2005; Angiboust et al., 2009; Groppo et al., 2009): This suggests that both units shared a common prograde-to-retrograde Alpine history and supports the pre-Alpine juxtaposition of the two units (Beltrando et al., 2010a).

The origin of chloritite

Chloritite is a relatively widespread rock type in metaophiolites of the western and central Alps. This lithology has been extensively studied for its archaeologic interest, having being used for the workability and fireproof characteristics to make pots, artistic objects and even stoves in the last 2000 years (Lepori et al., 1986; Lhemon and Serneels, 2012). In the archaeologic literature, chloritite is known as "*pietra ollare*" (*soapstone p.p.* in English) and includes a number of greenish and soft lithologies classified microscopically by Mannoni and Messiga (1980), Mannoni et al. (1987) and Castello and De Leo (2007). From field evidence and trace elements and isotopic data, chloritites appear to derive from replacement
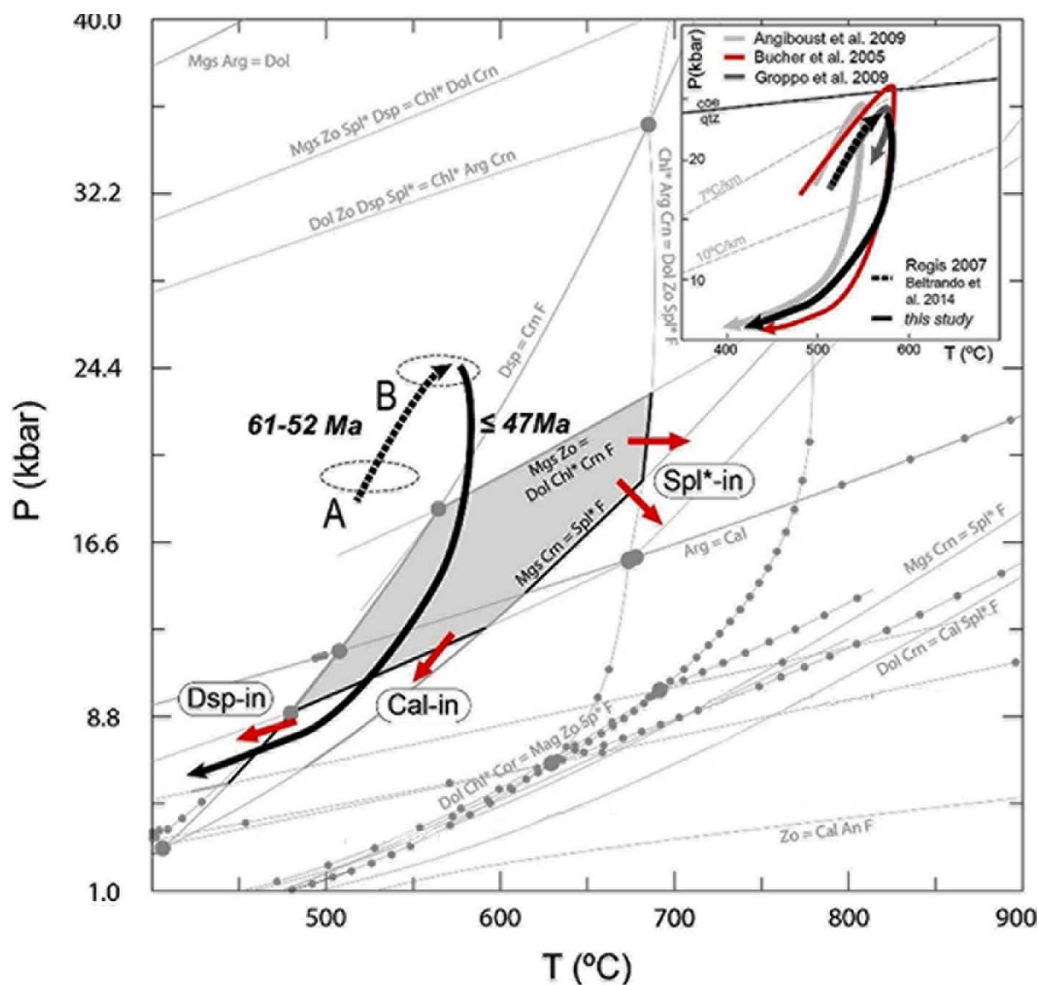
Fig. 11 - Reconstructed P-T-(t) path for the Alpine metamorphic evolution of the ELS based on this study and unpublished data of Regis (2007). The prograde path (stages A and B) was estimated by clinopyroxene-garnet-phengite thermobarometry in eclogites collected within the eclogitic micaschists of the Etirol-Levaz continental slice (Regis, 2007). The retrograde path ($t \leq 47$-45 Ma ago) was reconstructed on the basis of Dol + Chl* + Crn + F forming reaction, Cal-in reaction (destabilizing dolomite) and Dsp-in reaction (destabilizing corundum). Thick black lines and red arrows indicate the Sp*-Cal- and Dsp-in reactions in P-T space. Reactions are written with the high temperature assemblage on the right of the equations.. In the inset: comparison of the reconstructed P-T path (*this study*) with unpublished data for the Etirol-Levaz slice (Regis, 2007) and published data for the Zermatt-Saas Zone (modified from Bucher et al., 2005; Angiboust et al., 2009; Groppo et al., 2009). Abbreviations as in Fig. 9.

of ultramafic and/or mafic protoliths, mainly belonging to the ophiolite suite (Reynes, 2016).

The absence of structural relics in the studied chloritite hampers an easy identification of the protolith. However, the preservation of relics of the zoned green spinel, a high-T mineral incompatible with chlorite, provides useful information. In particular, the green spinel GS1 has an average chemical composition ($Sp_{58}Hc_{42}$) similar to that of the igneous green spinel (Sp_{66} and Hc_{32}) from an undeformed *cumulus websterite* of the "*Gabbros de Levaz*" (Fig. 1) reported by Kienast (1983). It is interesting to note that this rock, rich in Al_2O_3 (28.08 wt%) and MgO (15.52 wt%) and poor in SiO_2 (31.51 wt%), has a bulk chemical composition ideal to produce by hydration a chloritite.

The partial re-equilibration of GS1 to GS2 is in agreement with the thermal metamorphic event observed in the studied gabbronorites and extensively described by Kienast (1983) in the rocks of the igneous layered complex. This thermal event, dated on geochronological basis by Beltrando et al. (2010b), resulted to be Permian in age. The presence of Mg-Blt inclusions only in the green spinel GS2 is consistent with the interpretation that this mineral, isostructural with magnesiohögbomite-2N3S, such as the other members of the högbomite supergroup, is also stable at relatively high-T.

The metasomatic process responsible for the hydration of websterite to chloritite must be post-Permian, and may have occurred during the Mesozoic mantle exhumation and/or during the Alpine orogenic cycle, two different geologic settings but both sharing water availability and circulation. The presence of the Alpine Crn + Chl + Dol veins favors the hypothesis that the majority if not the whole hydration process developed during the early stages of the Alpine evolution, most likely ≤ 47-45 Ma ago (Fig. 11), as inferred by Dal Piaz et al. (2001) and Beltrando et al. (2010a) on geochronological basis.

CONCLUSIONS

The studied chloritite veins from the Etirol-Levaz Slice report the first occurrence of corundum in a mafic/ultramafic layered complex of the Western Italian Alps. The study of the chloritite, combined with the unpublished data of Regis (2007) from eclogites of the Etirol-Levaz continental crust, has allowed the entire prograde, HP-peak and retrograde Alpine P-T-path of to be reconstructed. The Alpine assemblage Crn + Chl + Dol formed about 47 My ago at ~ 17-15 kbar and ~ 580ºC, during the retrograde decompression subsequent to the HP eclogite-facies peak estimated to have occurred at about 560ºC and 24 kbar. The crystallization of this Alpine assemblage was triggered by the circulation of a hydrous fluid phase with very low $X_{(CO2)}$ (≤ 0.04).

The pre-Alpine thermal event, described by Kienast (1983) and confirmed by our observations (re-equilibration of relict igneous green spinel GS1 into GS2 in chloritites, and granoblastic recrystallization of Cpx in metagabbronorites), is consistent with the pre-Alpine history inferred on geochronological basis who found the cores of Permian magmatic zircons systematically overgrown by a Jurassic rim (166-150 Ma). This event, interpreted by Beltrando et al. (2010a) as due to melt infiltration associated with rift-related gabbroic magmas, is responsible for the thermal metamorphism already described by Kienast (1983).

REFERENCES

Abart R., Connolly J.A.D. and Trommsdorff V., 1992. Singular point analysis: construction of Schreinemakers projections for systems with a binary solution. Am. J. Sci., 292: 778-805.

Armbruster T., 2002. Revised nomenclature of högbomite, nigerite, and taaffeite minerals. Eur. J. Miner., 14: 389-395.

Baker J., Holland T. and Powell R., 1991. Isograds in internally buffered systems without solid solutions: principles and examples. Contrib. Miner. Petrol., 106: 170-182.

Ballèvre M., Kienast J.-R. and Vuichard J.P. 1986. La nappe de la Dent-Blanche (Alpes occidentales) : Deux unités austroalpines indépendantes. Ecl. Geol. Helv., 79: 57-74.

Beltrando M., Compagnoni R., Barnes J., Frezzotti M.L., Regis D., Frasca G., Forster M. and Lister G., 2014. From passive margins to orogens: The link between zones of Exhumed Continental Mantle and (U)HP metamorphism. - The UHP Lago di Cignana Unit, Zermatt-Saas Zone. 10th Int. Eclogite Conference, Pre-Conference Excursion, Day 2, September 2013, GFT - Geo. Field Trips, 6 (1.1): 33-53. ISSN: 2038-4947.

Beltrando M., Compagnoni R. and Lombardo B., 2010a. (Ultra-) High-pressure metamorphism and orogenesis: An Alpine perspective. Gondw. Res., 18: 147-166.

Beltrando M., Rubatto D. and Manatschal G., 2010b. From passive margins to orogens: The link between Ocean-Continent Transition zones and (Ultra-)High-Pressure metamorphism. Geology, 38 (6): 559-562.

Braga R., Callegari A., Messiga B., Ottolini L., Renna M.R. and Tribuzio R., 2003. Origin of prismatine from the Sondalo granulites (Central Alps, northern Italy). Eur. J. Miner., 15: 393-400.

Bosi F., Biagioni C. and Pasero M., 2019. Nomenclature and classification of the spinel supergroup. Eur. J. Miner., 31: 183-192.

Bucher K., Fazis Y., De Capitani C. and Grapes R., 2005. Blueschists, eclogites, and decompression assemblages of the Zermatt-Saas ophiolite: high-pressure metamorphism of subducted Tethys lithosphere. Am. Miner., 90: 821-835.

Bucher-Nurminen K., Frank E. and Frey M., 1983. A model for the progressive regional metamorphism of margarite-bearing rocks in the Central Alps. Am. J. Sci., 283 (A): 370-395.

Cámara F., Cossio R., Regis D., Cerantola V., Ciriotti M.E. and Compagnoni R., 2018. Beltrandoite, a new root-name in the högbomite supergroup: The Mg-end member magnesiobeltrandoite-2N3S. Eur. J. Miner., 30: 545–558.

Carmichael D.M., 1991. Univariant mixed-volatile reactions: pressure-temperature phase diagrams and reaction isograds. Can. Miner., 29: 741-754.

Cartwright I. and Barnicoat A.C., 2002. Petrology, geochronology, and tectonics of shear zones in the Zermatt-Saas and Combin zones of the Western Alps. J. Metam. Geol., 20 (2): 263-281.

Castelli D., Rolfo F., Groppo C. and Compagnoni R., 2007. Impure marbles from the UHP Brossasco- Isasca Unit (Dora-Maira Massif, western Alps): evidence for Alpine equilibration in the diamond stability field and evaluation of the X(CO$_2$) fluid evolution. J. Metam. Geol., 25: 587-603.

Castello P. and De Leo S., 2007. Pietra ollare della Valle d'Aosta: caratterizzazione petrografica di una serie di campioni ed inventario degli affioramenti, cave e laboratori. Bull. Études Préhistor. Archéol. Alpines, Aoste, 18: 53-75.

Connolly J.A.D., 1990. Multivariable phase diagrams; an algorithm based on generalized thermodynamics. Am. J. Sci., 290: 666-718.

Connolly J.A.D. and Trommsdorff V., 1991. Petrogenetic grids for metacarbonate rocks: pressure-temperature phase-diagram projection for mixed-volatile systems. Contrib. Mineral. Petrol., 108 (1-2): 93-105.

Dal Piaz G.V., 1999. The Austroalpine-Piedmont nappe stack and the puzzle of Alpine Tethys. In: G. Gosso et al. (Eds.), 3rd Workshop on Alpine geological studies, Biella-Oropa, September - October 1997. Mem. Sci. Geol. (Padua), 51: 155-176.

Dal Piaz G.V. and Ernst W.G., 1978. Areal geology and petrology of eclogites and associated metabasites of the Piemonte Ophiolite Nappe, Breuil-St. Jacques area, Italian Western Alps. Tectonophysics, 5: 99-126.

Dal Piaz G.V., Cortiana G., Del Moro A., Martin S., Pennacchioni G. and Tartarotti P., 2001. Tertiary age and paleostructural inferences of the eclogitic imprint in the Austroalpine outliers and Zermatt-Saas ophiolite, western Alps. Int. J. Earth Sci., 90: 668-684.

Emmett J.L., Scarratt K., McClure S.F., Moses T., Douthit T.R., Hughes R., Novak S., Shigley J.E., Wang W., Bordelon O. and Kane R.E., 2003. Beryllium diffusion of ruby and sapphire. Gems Gemol., 39 (2): 84-135.

Fettes D. and Desmons J., 2007. Metamorphic rocks. A classification and glossary of terms. Cambridge Univ. Press, 244 pp.

Gabudianu Radulescu I., Rubatto D., Gregory C. and Compagnoni R., 2009. The age of HP metamorphism in the Gran Paradiso Massif, Western Alps: A petrological and geochronological study of "silvery micaschists". Lithos, 110: 95-108.

Gaft M., Reisfeld R. and Panczer G., 2005. Modern luminescence spectroscopy of minerals and materials, Springer, Berlin, 356 pp.

Girardeau J. and Gil Ibarguchi J.I., 1991. Pyroxenite-rich peridotites of the Cabo Ortegal complex (Northwestern Spain): evidence for large-scale upper-mantle heterogeneity. J. Petrol., 32: 135-154.

Giuliani G., Ohnenstetter D., Garnier V., Fallick A.E., Rakotondrazafny M. and Schwarz D., 2007. The geology and genesis of gem corundum deposits. In: L.A. Groat (Ed.), Geology of gems deposits, Miner. Ass. Can., Short Course Ser., 37: 23-78.

Grew E.S., Drugova G.M. and Leskova N.V., 1989. Högbomite from the Aldan Shield, Eastern Siberia, USSR. Miner. Mag., 53: 376-379.

Groppo C., Beltrando M. and Compagnoni R., 2009. *P-T* path of the UH*P* Lago di Cignana and adjoining HP meta-ophiolitic units: insights into the evolution of the subducting Tethyan slab. J. Metam. Geol., 27: 207-231.

Groppo C., Castelli D. and Rolfo F., 2007. HT, pre-Alpine relics in a spinel-bearing dolomite marble from the UHP Brossasco-Isasca Unit (Dora-Maira Massif, western Alps, Italy). Per. Miner., 76: 155-168.

Habler G. and Thöni M., 2001. Preservation of Permo-Triassic low-pressure assemblages in the Cretaceous high-pressure metamorphic Saualpe crystalline basement (Eastern Alps, Austria). J. Metam. Geol., 19: 679-697.

Hejny C. and Armbruster T., 2002. Polysomatism in högbomite: The crystal structures of 10T, 12H, 14T, and 24R polysomes. Am. Miner., 87: 277-292.

Hermann F., 1938. Carta Geologica delle Alpi nord-occidentali alla scala 1:200,000, con note illustrative e carta strutturale alla scala 1 to 750,000. Arti Grafiche Moreschi and Co., Milano, Ufficio Cartografico S.A.C.A.R.T.A., Milano.

Hey M.H., 1954. A new review of the chlorites. Miner. Mag., 30: 277-292.

Holland T.J.B. and Powell R., 1998. An internally consistent thermodynamic data set for phases of petrologic interest. J. Metam. Geol., 16: 309-343.

Kienast J.-R. 1983. Le métamorphisme de haute pression et basse température (éclogites et schistes bleus) : données nouvelles sur la pétrologie des roches de la croûte océanique subductée et des sédiments associés. PhD Thesis, N° 83-49, Univ. P. et M. Curie, Paris 6, 532pp.

Konzett J., Miller C., Armstrong R. and Thöni M., 2005. Metamorphic evolution of iron-rich mafic cumulates from the Ötztal-Stubai Crystalline Complex, Eastern Alps, Austria. J. Petrol., 46: 717-747.

Kornprobst J., Piboule M., Roden M. and Tabit A., 1990. Corundum-bearing garnet clinopyroxenites at Beni Bousera (Morocco): original plagioclase-rich gabbros recrystallized at depth within the mantle? J. Petrol., 31: 717-745.

Lepori M, Donati B., Gaggioni A., Donati P.A., Pfeifer H.R. and Serneels V., 1986. 2000 anni di pietra ollare. Quaderni di informazione. Dipart. Ambiente, Uff. cantonale monumenti storici, Bellinzona (Svizzera), 235pp.

Lhemon M. and Serneels V., 2012. (Eds.) Pierre Ollaire. Actes de la Table Ronde, septembre 2008. Musée de la Pierre Ollaire de Champsec (commune de Bagnes / Valais / Suisse). Minaria Helv. Bull. Soc. Suisse d'Histoire des Mines, 30, 132pp.

Liati A. and Seidel E., 1994. Sapphirine and högbomite in overprinted kyanite-eclogites of central Rhodope, N. Greece: first evidence of granulite-facies metamorphism. Eur. J. Miner., 6: 733-738.

Liati A. and Seidel E., 1996. Metamorphic evolution and geochemistry of kyanite eclogites in central Rhodope, northern Greece. Contrib. Miner. Petrol., 123: 293-307.

Mannoni T. and Messiga B., 1980. La produzione e la diffusione dei recipienti di pietra ollare nell'Alto Medioevo. Atti del 6° Congr. Int. Studi sull'Alto Medioevo, Spoleto, p. 501-522

Mannoni T., Pfeifer H.R. and Serneels V. 1987. Giacimenti e cave di pietra ollare nelle Alpi. Atti Convegno "La pietra ollare dalla preistoria all'età moderna", (Como, ottobre 1982). New Press: Como, p. 7-45.

Morishita T., Arai S. and Gervilla F., 2001. High-pressure aluminous mafic rocks from the Ronda peridotite massif, southern Spain: significance of sapphirine- and corundum-bearing mineral assemblages. Lithos, 57: 143-161.

Müntener O. and Hermann J., 1996. The Val Malenco lower crust - upper mantle complex and its field relations (Italian Alps). Schweiz. Miner. Petrogr. Mitt., 76: 475-500.

Newton R.C. and Manning C.E., 2008. Solubility of corundum in the system Al_2O_3-SiO_2-H_2O-NaCl at 800°C and 10 kbar. Chem. Geol., 249: 250-261.

Omori S., Liou J.G., Zhang R.Y. and Ogasawara Y., 1998. Petrogenesis of impure dolomitic marble from the Dabie Mountains, central China. Island Arc, 7 (1-2): 98-114.

Petersen E.U., Essene E.J., Peacor D.R. and Marcotty L.A., 1989. The occurrence of högbomite in high-grade metamorphic rocks. Contrib. Miner. Petrol., 101: 350-360.

Razakamanana T., Ackermand D. and Windley B.F., 2000. Högbomite in migmatitic paragneiss in the Betroka shear belt, Vohidava area, Precambrian of southern Madagascar. Miner. Petrol., 68: 257-269.

Regis D., 2007. The Austroalpine slice of Etirol-Levaz (Valtournenche, Valle d'Aosta): new data on the prograde metamorphic path and eclogite-facies peak. Unpubl. MSc Thesis, Univ Torino (in Italian), 98 pp.

Regis D., Cossio R. and Compagnoni R., 2015. Alpine corundum-bearing veins from the Etirol-Levaz austroalpine continental slice (Valtournenche, Aosta, Italy). Rend. Online Soc. Geol. It., 37: 57-60, doi: 10.3301/ROL.2015.182

Reynes J., 2016. Circulation de fluides et métasomatisme du plancher océanique à la zone de subduction : le cas des chloritites alpines. IPGP-IMPMC, Mém. de Master 2, 30pp.

Riesco M., Stüwe K. and Reche J., 2005. Formation of corundum in metapelites around ultramafic bodies. An example from the Saualpe region, Eastern Alps. Miner. Petrol., 83: 1-25.

Sengupta P., Raith M.M. and Levitsky V.I., 2004. Compositional characteristics and paragenetic relations of magnesiohögbomite in aluminous amphibolites from the Belomorian complex, Shield, Russia. Am. Miner., 89: 819-831.

Sengupta P., Bhui U.K., Braun I., Dutta U. and Mukhopadhyay D., 2009. Chemical substitutions, paragenetic relations, and physical conditions of formation of högbomite in the Sittampundi layered anorthosite complex, South India. Am. Miner., 94: 1520-1534.

Simonet C., Fritsch E. and Lasnier B., 2008. A classification of gem corundum deposits aimed towards gem exploration. Ore Geol. Rev., 34: 127-133.

Tsunogae T. and Santosh M., 2005. Ti-free högbomite in spinel- and sapphirine-bearing Mg-Al rock from the Palghat-Cauvery shear zone system, southern India. Miner. Mag., 69 (6): 937-949.

Yakymchuk C. and Szila K. 2018. Corundum formation by metasomatic reactions in Archean metapelite, SW Greenland: Exploration vectors for ruby deposits within high-grade greenstone belts. Geosci. Front., 9: 727-749.

Yalçin Ü., Schreyer W. and Medenbach O., 1993. Zn-rich högbomite formed from gahnite in the metabauxites of the Menderes Massif, SW Turkey. Contrib. Miner. Petrol., 113: 314-324.

Zhang R.Y., Liou J.G. and Zheng J.P., 2004. Ultrahigh-pressure corundum-rich garnetite in garnet peridotite, Sulu terrane, China. Contrib. Miner. Petrol., 147: 21-31.